Supplemental Information for

In vivo measurement of granzyme proteolysis from activated immune cells with PET

Ning Zhao[1,#], Conner Bardine[2,#], André Luiz Lourenço[2], Yung-hua Wang[1], Yangjie Huang[1], Simon J. Cleary[3,4], David M. Wilson[1], David Y. Oh[3,5], Lawrence Fong[3,5], Mark R. Looney[3,4], Michael J. Evans[1,2,5,*], Charles S. Craik[2,5,*]

[1]Department of Radiology and Biomedical Imaging, [2] Department of Pharmaceutical Chemistry, [3]Department of Medicine, [3]Department of Laboratory Medicine, [4]Department of Radiation Oncology, [5]Helen Diller Family Comprehensive Cancer Center, University of California San Francisco, San Francisco, CA 94143.

#Co-first authors

*To whom correspondences should be addressed:

Michael J. Evans, PhD
Associate Professor
michael.evans@ucsf.edu
Tel: 415-514-1292

Charles S. Craik, PhD
Professor
charles.craik@ucsf.edu
Tel: 415-476-8146

Supplemental Figure 1. A heat map showing the preferred cleavage sites for recombinant human granzyme B as predicted with multisubstrate profiling mass spectrometry where 1-8 represents P4-P4', respectively.

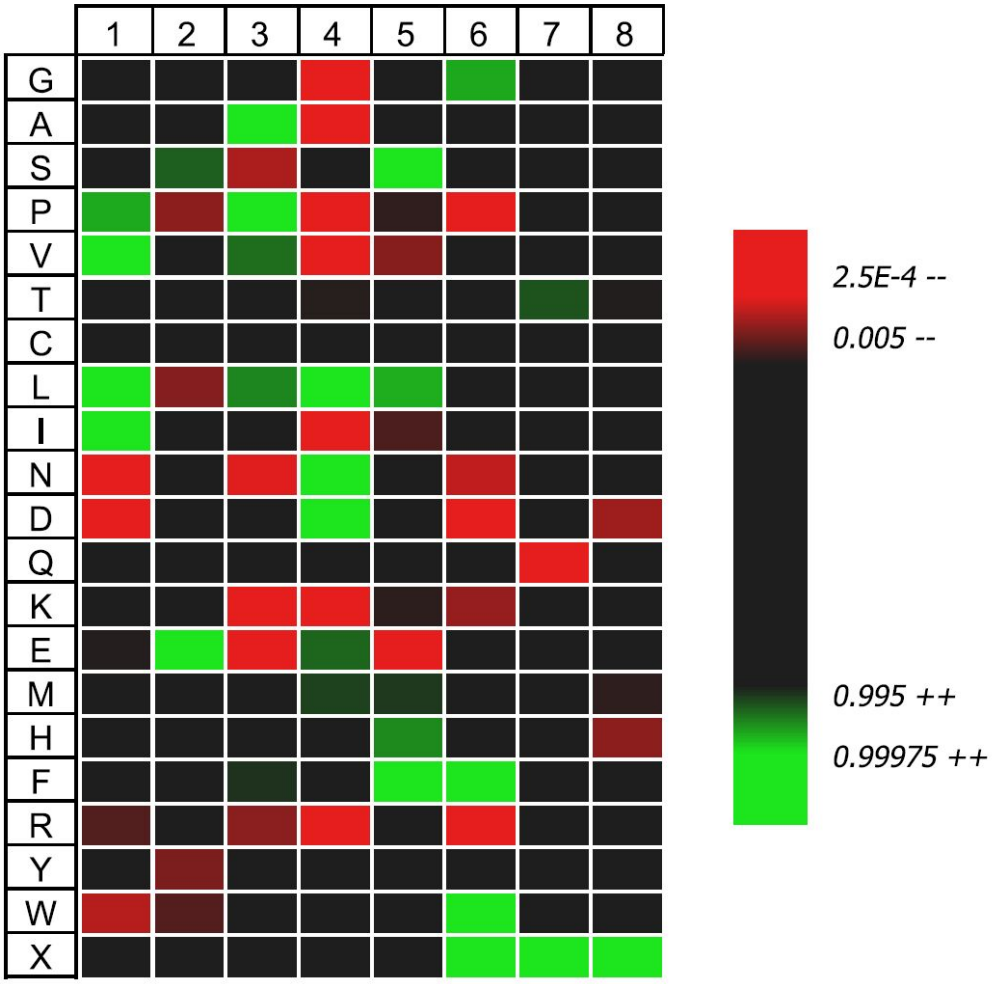

Supplemental Figure 2. Stacked HPLC traces showing the cleavage of GRIP B by recombinant human GZMB. The single product peak at ~7.7 minutes comigrates with the peptide standard FVQWFSKFLGKIEPD. The data are reflective of three independent experiments.

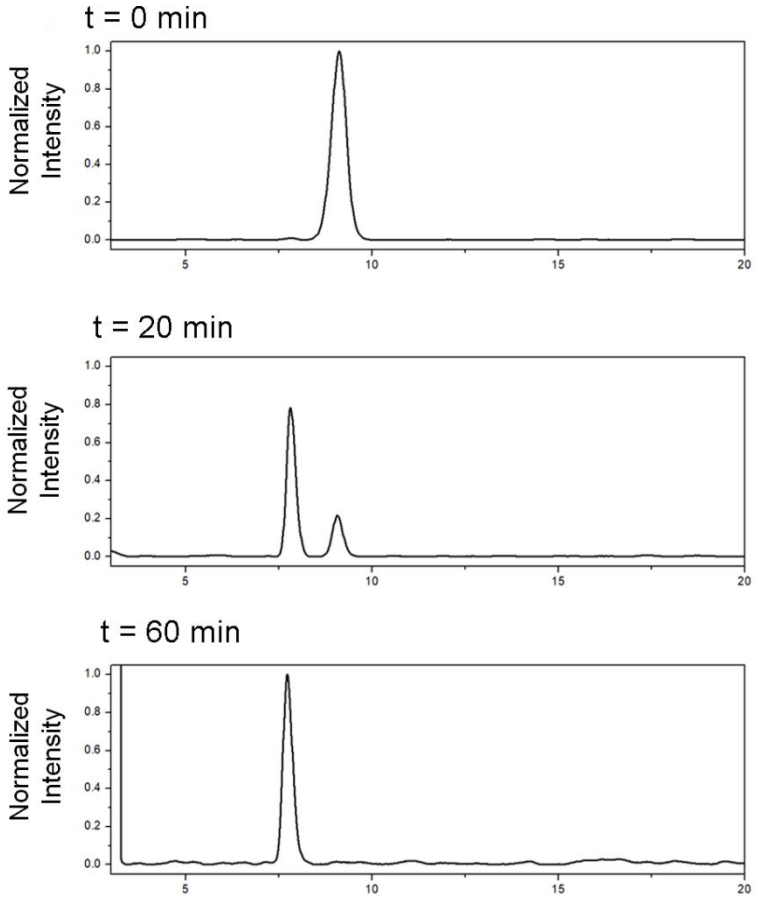

Supplemental Figure 3. Tryptophan insertion experiments and circular dichroism.
A. Probing membrane interaction dynamics with SDS-micelles through tryptophan intrinsic fluorescence reveals partial interaction of the full-length propeptide, and complete internalization of the activated GRIP B. **B.** Circular dichroism of full-length GRIP B shows a spectrum indicative of a disordered peptide, suggesting that the masking domain is effective in disrupting the alpha helical secondary structure of the cell penetrating peptide module. **C.** Circular dichroism of activated GRIP B reveals the characteristic spectra of alpha helical peptides, showing that the probe retains the secondary structure of Temporin L.

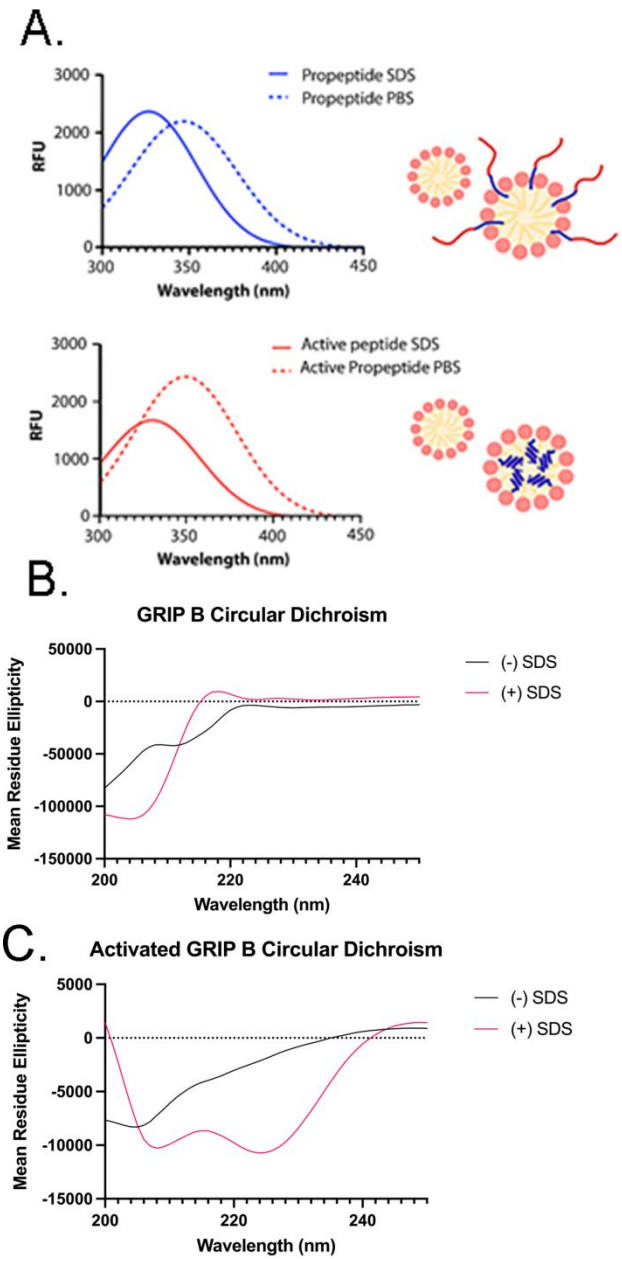

Supplemental Figure 4. The structure of DOTA-GRIP B.

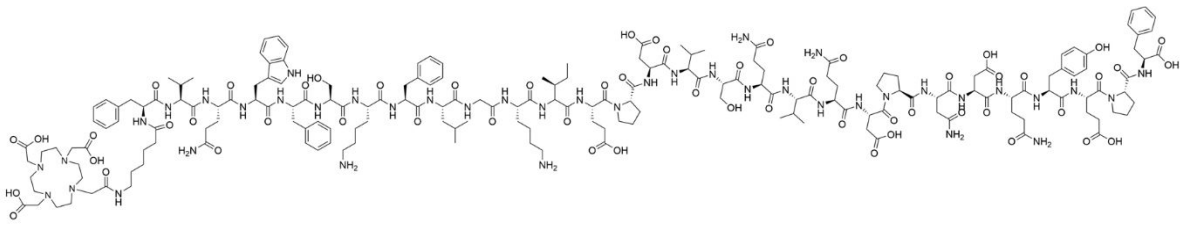

Supplemental Figure 5. A plot showing the stability of ^{64}Cu-GRIP B in mouse serum. The probe was incubated at 37° C, and the radioactive species were separated and quantified on RAD-HPLC.

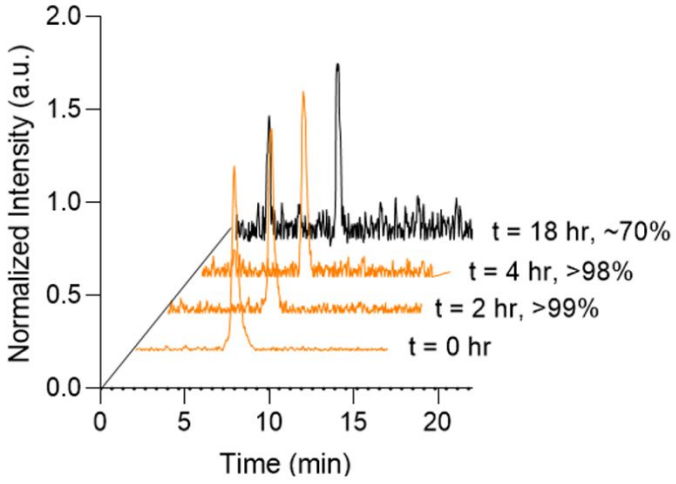

Supplemental Figure 6. An example of a compartmental analysis of tumoral uptake of ^{64}Cu-GRIP B. The analysis was performed using a 1 hour dynamic PET acquisition from a Balb/c mouse bearing a MC38 tumor with was treated with CPI. The analysis show $k_3 > k_4$ and $k_4 \sim 0$. These data are representative of similar outcomes for C57Bl6 mice bearing CT26 tumors.

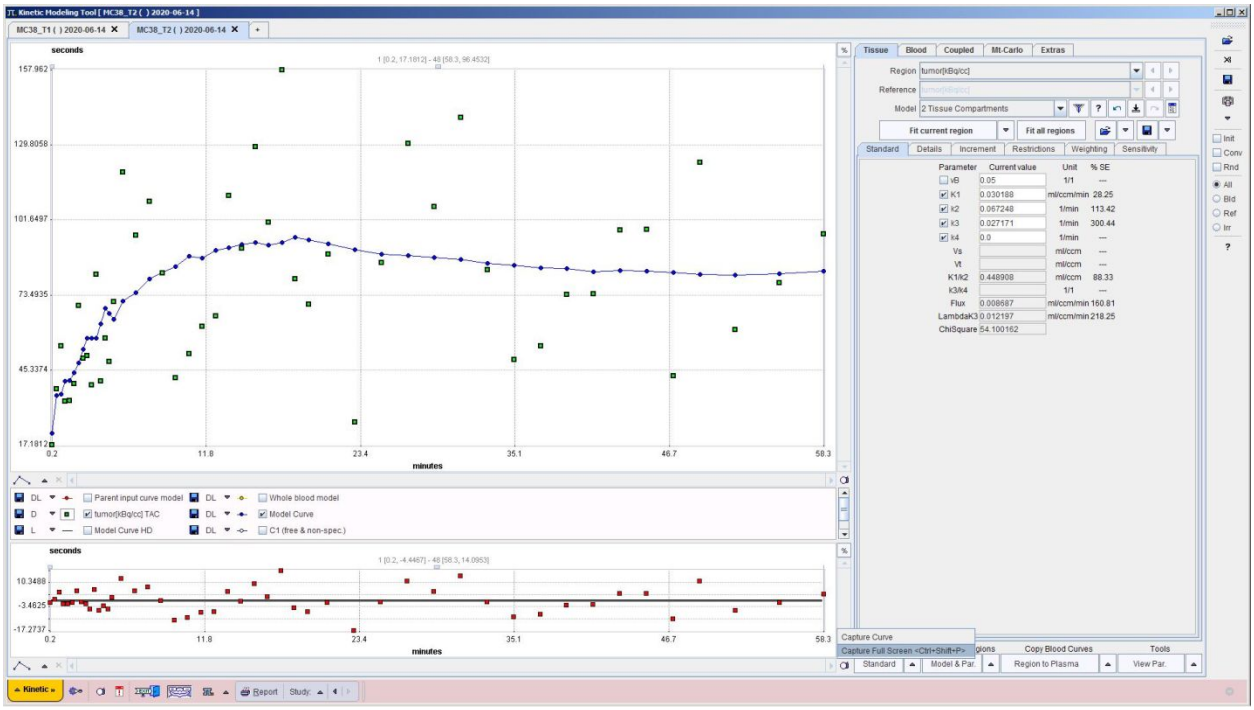

Supplemental Figure 7. Representative coronal ^{64}Cu-GRIP B PET/CT images of mice bearing CT26 tumors and treated with vehicle or checkpoint inhibitors. The position of the CT26 tumor is indicated with an orange arrow.

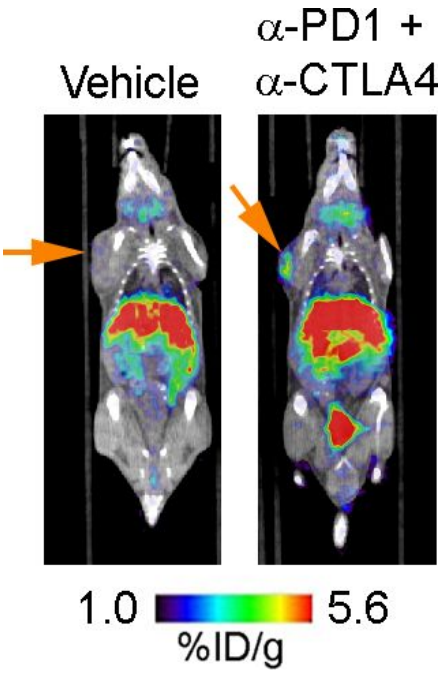

Supplemental Figure 8. Analytical HPLC data showing the synthesis of ^{64}Cu-D-GRIP B. The blue trace shows the RAD peak from the complex reaction mixture. The black peak shows the UV of the DOTA-D-GRIP B starting material.

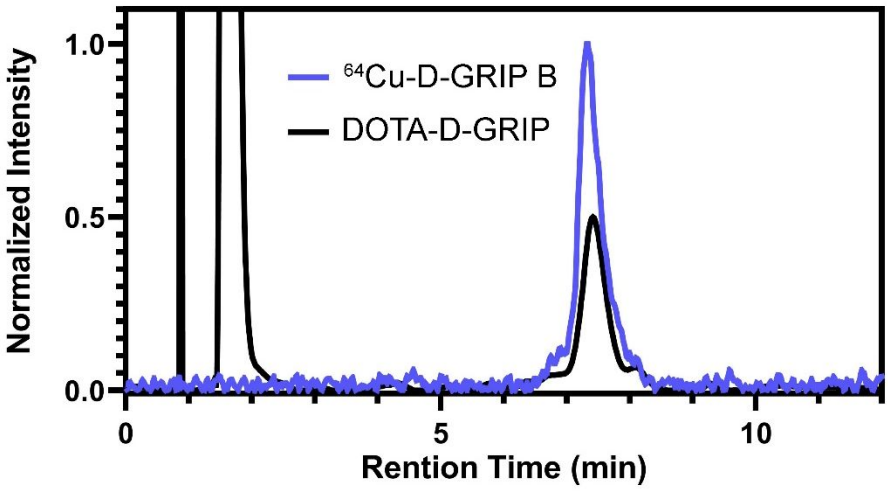

Supplemental Figure 9. Immunofluorescence data showing increased staining for the neutrophil marker Ly6G in LPS versus vehicle treated lung tissue. No obvious difference was observed between arms in the intensity of the natural killer cell marker NKp46/NCR1. The stained slides were adjacent to the slices shown in Figure 6.

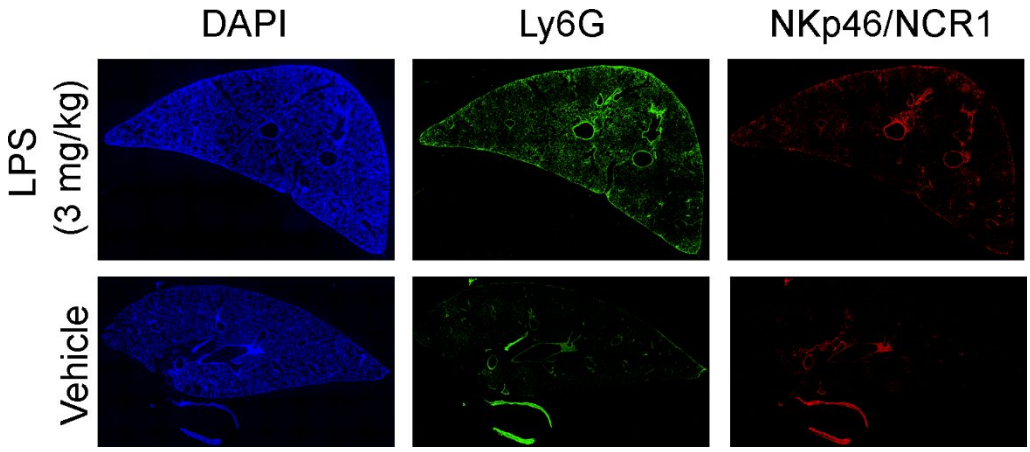

Supplemental Table 1. A tabular representation of the biodistribution data collected at various time points post injection of ^{64}Cu-GRIP B in tumor naïve male C57BL/6 mice. The data represent the mean ± standard deviation, n = 4 per time point.

Tissue	Time post injection (hr)				
	0.5	**1**	**2**	**4**	**24**
Blood	4.58 ± 0.3	3.07 ± 1.3	1.55 ± 0.1	1.61 ± 0.2	1.15 ± 0.06
Brain	0.33 ± 0.06	0.31 ± 0.02	0.32 ± 0.02	0.39 ± 0.03	0.43 ± 0.02
Heart	3.07 ± 0.3	2.49 ± 0.4	2.22 ± 0.2	2.62 ± 0.2	2.73 ± 0.3
Liver	16.94 ± 1.1	20.38 ± 2.2	24.98 ± 2.7	22.78 ± 1.3	21.56 ± 1.6
Kidneys	148.36 ± 7.9	90.35 ± 7.2	54.39 ± 9.5	54.16 ± 12.6	14.58 ± 3.3
Spleen	2.72 ± 0.3	2.92 ± 0.6	2.22 ± 0.3	2.42 ± 0.8	2.07 ± 0.09
Pancreas	1.67 ± 0.1	1.84 ± 0.8	1.77 ± 0.6	1.49 ± 0.2	1.54 ± 0.08
Stomach	2.83 ± 0.9	3.24 ± 0.7	4.28 ± 0.4	3.72 ± 1.5	3.27 ± 0.2
Small Intestine	8.4 ± 0.07	11.08 ± 1.9	8.14 ± 0.8	9.98 ± 1.7	6.15 ± 0.8
Large Intestine	4.64 ± 0.2	5.64 ± 0.8	10.69 ± 3.1	13.78 ± 1.3	6.8 ± 0.9
Skeletal Muscle	1.19 ± 0.1	1.17 ± 0.3	0.75 ± 0.1	0.66 ± 0.07	0.67 ± 0.06
Bone	1.86 ± 0.4	1.45 ± 0.3	1.21 ± 0.01	1.46 ± 0.3	1.29 ± 0.1
Lung	5.81 ± 0.8	5.81 ± 0.7	6.88 ± 0.2	7.43 ± 0.7	6.72 ± 0.6
Thymus	2.49 ± 0.3	2.43 ± 0.2	2.2 ± 0.1	2.48 ± 0.5	2.67 ± 0.4
Brown Fat	3.34 ± 0.4	2.2 ± 0.2	2.93 ± 0.5	3.25 ± 0.8	3.15 ± 0.7
White Fat	0.97 ± 0.5	0.46 ± 0.09	0.47 ± 0.1	0.3 ± 0.04	0.33 ± 0.1

Supplemental Table 2. A summary of the SUVmean values acquired from region of interest analysis of dynamic PET acquisitions. The data are reported as SUVmean ± standard deviation.

Time (sec)	Control		CPI	
	SUV_{mean}	SD	SUV_{mean}	SD
10	0.03	0.3	0.11	0.3
30	0.29	0.7	0.67	1.3
50	0.49	1.2	0.24	0.6
70	0.67	1.6	2.27	2.4
110	1.04	2.1	2.77	3.7
130	0.49	0.8	2.46	3.0
150	0.55	1.0	2.28	3.3
170	1.19	1.9	2.32	3.9
210	1.02	1.9	2.58	3.0
270	0.81	1.5	3.29	4.4
330	0.88	1.1	2.56	1.8
390	0.75	1.1	3.20	3.1
450	0.60	1.0	2.95	2.4
510	0.74	1.4	4.11	4.7
570	0.86	1.3	3.70	3.3
630	0.75	0.9	4.73	3.3
690	1.14	1.8	3.88	2.8
750	1.06	1.5	3.21	2.5
810	0.72	1.1	3.55	2.7
870	0.66	0.8	3.87	2.6
990	1.06	1.5	4.01	2.5
1050	0.86	0.9	3.46	3.7
1110	0.70	1.1	4.42	2.8
1170	1.17	1.6	3.82	2.8
1260	1.04	1.3	4.86	2.3
1380	0.59	0.7	3.89	2.3
1500	1.10	1.0	4.65	2.3
1620	0.72	0.7	4.57	2.4
1740	1.25	1.1	3.69	1.9
1860	0.84	0.8	4.51	2.4
1980	1.31	1.2	4.27	1.9
2220	1.20	1.1	4.98	2.2
2340	1.11	0.9	5.34	2.8
2580	1.11	1.1	4.91	3.2
2700	0.98	1.2	4.66	2.5
2820	1.21	1.1	4.63	2.3
3100	1.46	1.3	4.76	1.7
3500	1.33	1.0	4.34	1.6

Supplemental Table 3. A tabular representation of the biodistribution data collected 2h post injection of radiotracer ^{64}Cu-L-GRIP B in male balb/c mice bearing CT26 tumor after receiving 3 antibody/PBS treatment. The P value indicates the result of an unpaired, two-tailed Student's t test between the two different arms (n = 8/group).

Tissue	Vehicle	CPI
Blood	0.55 ± 0.05	0.56 ± 0.02
Brain	0.12 ± 0.02	0.12 ± 0.01
Heart	1.53 ± 0.8	1.32 ± 0.4
Liver	8.54 ± 0.8	8.15 ± 1.4
Kidneys	34.51 ± 4.9	33.83 ± 7.1
Spleen	0.89 ± 0.3	1.62 ± 1.1
Pancreas	1.44 ± 1.3	1.07 ± 0.4
Stomach	1.68 ± 0.9	1.66 ± 0.6
Small Intestine	3.96 ± 0.6	4.28 ± 1.3
Large Intestine	4.48 ± 1.4	3.8 ± 1.1
Muscle	0.39 ± 0.1	0.35 ± 0.1
Bone	0.53 ± 0.1	0.54 ± 0.1
Lung	3.53 ± 1.5	3.76 ± 2.2
Tumor	1.73 ± 0.4	2.43 ± 0.5

Supplemental Table 4. Biodistribution data collected 2 hours post injection of ^{64}Cu-D-GRIP B in male C57Bl6 mice bearing MC38 tumors. The data are expressed as mean %ID/g ± standard deviation, n = 8 per treatment arm.

Tissue	Vehicle	Treatment
Blood	1.10 ± 0.2	1.0 ± 0.2
Brain	0.19 ± 0.05	0.21 ± 0.09
Heart	1.38 ± 0.1	1.2 ± 0.08
Liver	13.18 ± 3.2	10.24 ± 3.5
Kidneys	34.28 ± 7.1	28.19 ± 2.2
Spleen	1.25 ± 0.2	1.24 ± 0.3
Pancreas	1.12 ± 0.8	0.91 ± 0.2
Stomach	2.36 ± 0.2	2.95 ± 0.8
Small Intestine	6.28 ± 2.1	6.57 ± 2.55
Large Intestine	4.54 ± 1.9	6.17 ± 2.5
Muscle	0.36 ± 0.1	0.42 ± 0.2
Bone	0.70 ± 0.1	0.82 ± 0.1
Lung	4.0 ± 0.5	3.84 ± 0.5
Tumor	2.29 ± 0.3	3.74 ± 1.2

Supplemental Table 5. Biodistribution data collected 2 hours post injection of ^{64}Cu-D-GRIP B in male C57Bl6 mice bearing MC38 tumors. The data are expressed as mean %ID/g ± standard deviation, n = 5 per treatment arm.

Tissue	Vehicle	CPI
Blood	1.21 ± 0.09	0.39 ± 0.03
Muscle	0.31 ± 0.06	0.21 ± 0.03
Spleen	1.06 ± 0.1	0.43 ± 0.02
Kidneys	34.10 ± 3.7	16.44 ± 2.5
Tumor	2.09 ± 0.2	2.22 ± 0.5

Supplemental Table 6. Biodistribution data collected 2 hours post injection of ^{64}Cu-GRIP B in female Balb6 mice bearing EMT6 tumors. The data are expressed as mean %ID/g ± standard deviation, n = 5 per treatment arm.

Tissue	Vehicle	CPI
Blood	0.55 ± 0.05	0.56 ± 0.02
Brain	0.12 ± 0.02	0.12 ± 0.01
Heart	1.53 ± 0.8	1.32 ± 0.44
Liver	8.54 ± 0.8	8.15 ± 1.42
Kidneys	34.51 ± 4.9	33.83 ± 7.16
Spleen	0.89 ± 0.34	1.62 ± 1.12
Pancreas	1.44 ± 1.39	1.07 ± 0.45
Stomach	1.68 ± 0.97	1.66 ± 0.65
Small Intestine	3.96 ± 0.63	4.28 ± 1.32
Large Intestine	4.48 ± 1.43	3.8 ± 1.11
Muscle	0.39 ± 0.19	0.35 ± 0.1
Bone	0.53 ± 0.17	0.54 ± 0.13
Lung	3.53 ± 1.54	3.76 ± 2.27
Tumor	1.83 ± 0.47	2.4 ± 0.59

Supplemental Table 7. Biodistribution data collected 2 hours post injection of ^{64}Cu-D-GRIP B in female Balb6 mice bearing EMT6 tumors. The data are expressed as mean %ID/g ± standard deviation, n = 5 per treatment arm.

Tissue	Vehicle	CPI
Blood	2.11 ± 0.12	1.29 ± 0.34
Muscle	0.36 ± 0.05	0.32 ± 0.04
Spleen	2.38 ± 0.19	1.83 ± 0.26
Kidneys	33.48 ± 3	41.7 ± 5.17
Tumor	1.55 ± 0.1	1.35 ± 0.21

Supplemental Table 8. Biodistribution data collected 2 hours post injection of ^{64}Cu-GRIP B in male or female *GZMB*-/- mice bearing CT26 tumors. The data are expressed as mean %ID/g ± standard deviation, n = 6 per treatment arm.

Tissue	Vehicle	CPI
Blood	0.84 ± 0.1	0.92 ± 0.1
Brain	0.10 ± 0.01	0.10 ± 0.04
Heart	0.97 ± 0.1	0.81 ± 0.4
Liver	8.12 ± 1.2	8.35 ± 1.6
Kidneys	30.50 ± 7.5	30.26 ± 4.5
Stomach	2.06 ± 1.0	2.02 ± 0.3
Small Intestine	4.91 ± 0.8	5.47 ± 1.1
Large Intestine	3.78 ± 1.6	2.61 ± 0.5
Skeletal Muscle	0.24 ± 0.05	0.36 ± 0.1
Bone	0.48 ± 0.09	0.49 ± 0.05
Pancreas	0.73 ± 0.5	0.76 ± 0.1
Spleen	0.68 ± 0.1	0.64 ± 0.1
Lung	2.62 ± 0.4	2.86 ± 0.4
Tumor	1.66 ± 0.3	1.74 ± 0.3

Supplemental Table 9. A summary of the biodistribution data acquired in C57Bl6 mice subjected to an intratracheal instillation of lipopolysaccharide at 0.1 or 3 mg/kg. The data are expressed as mean %ID/g ± standard deviation, n = 5 per treatment arm.

Tissue	Vehicle	LPS (0.1 mg/kg)	LPS (3 mg/kg)
Blood	0.73 ± 0.01	0.71 ± 0.07	1.19 ± 0.2
Brain	0.11 ± 0.02	0.11 ± 0.01	0.21 ± 0.02
Heart	1.09 ± 0.1	1.29 ± 0.3	1.66 ± 0.2
Liver	9.81 ± 0.5	8.65 ± 0.7	15.3 ± 1.0
Kidneys	20.58 ± 2.9	20.32 ± 4.2	35.26 ± 2.7
Spleen	0.77 ± 0.3	0.76 ± 0.1	1.38 ± 0.2
Pancreas	1.13 ± 0.09	1.13 ± 0.07	1.5 ± 0.1
Stomach	2.98 ± 0.7	2.39 ± 0.5	2.53 ± 0.2
Small Intestine	4.49 ± 0.5	4.37 ± 0.6	6.52 ± 0.3
Large Intestine	4.13 ± 2.7	2.81 ± 0.2	4.45 ± 1.1
Muscle	0.39 ± 0.1	0.26 ± 0.02	0.36 ± 0.04
Bone	0.73 ± 0.1	0.50 ± 0.1	0.71 ± 0.07
Lung	3.64 ± 0.2	3.41 ± 0.3	4.14 ± 0.09
Thymus	1.18 ± 0.07	1.22 ± 0.2	4.18 ± 0.6